

An Electromagnetic Inverse Problem in the Medical Sciences

By

Preston Sturkie

A Thesis Submitted in Partial Fulfillment

Of the Requirements for the Degree

Master of Science

Major Subject: Mathematics

West Texas A&M University

Canyon, Texas

August 2019

ABSTRACT

Most human tissue is heavily comprised of water and ions; which is dispersive of electromagnetic energy. The definitive goal of this research is to make an accurate determination of dielectric constants and conductivity at different given frequencies of living tissue from measurements outside of the human body. Previous studies used tissue samples or probing mechanisms, but these methods to deduce both the dielectric constant and conductivity values are not necessarily reproducible since the sample itself is not in its natural environment. In the future, the overall goal would be to illuminate the human body with a broad-band pulse of electromagnetic radiation. By doing so, one could measure the dielectric constants or conductivities throughout the body by accumulating reflected and/or transmitted signals. Thus may one deductively determine the electrical coefficients through the use of an inverse problem using the incident and scattered fields as a function of position within the body.

The process and technique implemented in this study uses a frequency response function. The inversion process is non-unique unless both the relative permittivity and conductivity are presumed to be differentiable as functions of frequency. The results, as expected, for the dielectric constant are fairly in accord to the true expected value. However, the conductivity values display much variation at the larger ranges of

frequency. This implies that the functions lose their authenticity as frequency is increased.

ACKNOWLEDGEMENTS

The author would like to thank Dr. Seth and committee members for their help, support and guidance.

Approved:

_____ Chairman, Thesis Committee	_____ Date
_____ Member, Thesis Committee	_____ Date
_____ Member, Thesis Committee	_____ Date
_____ Department Head/Direct Supervisor	_____ Date
_____ Dean, Academic College	_____ Date
_____ Dean, Graduate School	_____ Date

TABLE OF CONTENTS

Section	Page
1: Introduction.....	1
Research Question	
Motivation for Research Question	
2: Background.....	5
3: The Inverse Problem Using a Frequency Response Function	9
4: Numerical Results for the Noiseless Case	15
5: Numerical Results with Noise	19
6: Conclusion	22
References.....	24

LIST OF TABLES

	Page
Table I.: Values of roots Alpha and Beta for the Frequency Response Function	10
Table II.: Values of X_n and Y_n at Given Frequencies	12
Table III.: Values of roots Alpha and Beta from Equation 15	14
Table IV.: Identification of Tissue Properties in Presence of Noise.....	19
Table V.: Identification of Tissue Properties in Presence of Noise	21

LIST OF FIGURES

	Page
Figure 1.A.: Relative Permittivity of Distilled Water at 10^4 Hertz	6
Figure 1.B.: Conductivity of Distilled Water at 10^8 Hertz	6
Figure 1.C.: Relative Permittivity of Distilled Water at 10^8 Hertz	7
Figure 1.D.: Conductivity of Distilled Water at 10^8 Hertz	7
Figure 2.A.: Relative Permittivity of the Noiseless Case at 10^4 Hertz	16
Figure 2.B.: Conductivity of the Noiseless Case at 10^4 Hertz	16
Figure 2.C.: Relative Permittivity of the Noiseless Case at 10^8 Hertz	17
Figure 2.D.: Conductivity of the Noiseless Case at 10^8 Hertz	17

1. INTRODUCTIION

Life in modern day America, especially in urban areas, produces quite a quantifiable amount of non-ionizing radiation within a broad band extending from below 60 Hz to above 10^{10} Hz. What is non-ionizing radiation? A rudimentary chemistry concept is that an ion has a net positive or negative electric charge due to the loss or gain of an electron. Therefore, a non-ionizing ion has a stable and more neutral net charge. Non-ionizing radiation does not carry enough energy to directly ionize an atom. Non-ionizing radiation is found at the long wavelength end of the spectrum. The longer the wavelength, measured in meters, the smaller the frequency value in hertz. When the frequency increases in value, so does the temperature of the bodies that is emitting the wavelength. An example of non-ionizing radiation, like a radio wave, has a wavelength value of approximately 10^3 meters. A micro wave has a frequency range of 10^4 to 10^8 Hertz. [23]. This type of radiation may have enough energy to excite molecules, and ionize atoms, causing them to vibrate faster, however, it does not have enough energy to directly damage DNA [15]. The continuous use of electrical power by the population enhances the exposure of radiaton at lower frequencies. The usage of the radio, television, radar and microwave ovens accounts more for mid-range and higher frequency exposure [1]. Since the public is constantly surrounded by the electrical grid, laptops,

microwaves, radar and other technological devices this investigation chose a frequency value of 10^4 and 10^8 Hertz.

Is this continuous and ever increasing exposure of radiation harmful to our health? The levels of non-ionizing radiation that occur in these particular frequency bands, especially those in inner-city regions, tend to be several orders of magnitude higher than compared to those that are found in nature [18, 20]. For years, this has been a question of concern and along with that of a possible link between electromagnetic fields produced from devices and inducing cancer [15]. Unremitting exposure of non-ionizing radiation has led to a vital medical question, “Are there any health consequences?” Even if there are not any serious and immediate health consequences, there is still a biological concern about the mechanisms of how nearby living organisms absorb and dissipate this type radiation. The human body has adaptive mechanisms for survival as the environment changes, whether that environment is natural or synthesized by humans. However, the body does not have adequate adaptive instruments for all biological interferences. The induced changes may constitute a health hazard as they add stress to the human system that could be irreversible over a long period of time [22].

Further research suggests one can use frequencies to shatter cancer cells. Matter is comprised of electrons. It is conceivable to disturb the electronic bonding through an application of frequencies, thus shattering the desired target. An example is the shattering of glass. Glass has a natural resonant frequency, the speed at which it vibrates if disturbed by some external source. If a singer can match the same frequency, the high pitch can produce vibrations strong enough to shatter glass. The potential to shatter cells was first demonstrated when a researcher used the correct combination of frequencies on

microorganisms; they broke apart [16]. Another example is Extracorporeal Shockwave Therapy. If a kidney stone is too large a medical doctor will use sound to produce vibrations in order to break the kidney stone down into its smaller components. In further experiments, the use of oscillating pulsed electric field technology led to the shatter of a percentage of leukemia cells.

Additionally, there may be probable beneficial uses in the medical sciences for the utilization of non-ionizing radiation if it is found that it will not harm the nearby healthy human tissue. An example of irradiation is thermalization. Thermalization is increasing the temperature. Adding more heat to a desired cell will denature its constituents, thus destroying the desired target. The proper use of thermalization to target cancerous cells may greatly aid in battling the disease, as long as this hyperthermic condition does not affect any of the nearby healthy tissues [9]. Hyperthermia may be implemented locally or regionally to target a desired entity as it heats a tumor. The nearby blood vessels and the cancer cells are demolished by using high temperature. There are different ways to apply this heat. One method is by aiming high energy waves at the tumor that is located close to the surface of the body. Another is allowing the heat to surround the sought after cancerous cell by releasing energy from a probe or needle [10]. Due to an increased metabolic rate, malignant tumors give off a higher temperature than do normal cells. Since a cancer cell's metabolic rate is faster it gives off a different frequency than normal cells. This difference in frequency could possibly lead to curing cancer by matching the cancer cell's frequency. Since the metabolic rate is faster in cancer cells increased radiation would also aid scientists to determine the cell's location. Scientists use this radiating heat source to locate its position with the use of infrared imaging. If the tumor is deep within the tissue, then

differentiation of a tumor from other inflamed cells can be problematic. Researchers have developed a way to increase the temperature in the tumor by using an external alternating magnetic field and magnetic nanoparticles, thus enhancing the imagery [21]. This is valuable to consider in mathematical research since one can use the electromagnetic radiation that is being produced from the cell in accord with thermalization.

Therefore, there is a dire need for research using electromagnetic wave propagation to beneficially corroborate the medical and biological sciences. For both health assessments and safety evaluations, it is crucial to calculate the electromagnetic fields that are occurring within the human body that are being exposed to these external sources of radiation. Due to the constant chemical reactions occurring in the human body, minuscule electrical currents exist, and these currents produce the electromagnetic fields [22]. One can calculate the fields by using a mathematical direct problem. A desire to implement thermalization on a desired tumor, while having insignificant thermalization to the nearby tissue, has led to a mathematical categorizing process for selecting the utmost influencing external sources [2].

To calculate the internal fields and to select optimal external sources requires the exact determination of the electrical coefficients of living tissue as a function of tissue type and the location within the tissue [1]. Due to previous tissue experiments, there is some data for both the dielectric constants and conductivities. However, these numerical values tend to be limited and not the most accurate since the human samples of tissue were either removed from living organisms, or were severely damaged by the insertion of probes into the trial samples [7, 17, 4]. Ergo, from either procedure, one can deduce that both the

relative permittivity and the conductivity values are questionable, since the sample tissue is not in its natural environment and function.

It is this investigation's objective to calculate accurate numerical values of both the dielectric constant and conductivities of tissue. This end is approached through the use of measurements outside of the living body through use of a frequency response function taken at two different frequencies of 10^4 and 10^8 Hertz. Finally, the future goal would be to illuminate the human body with a broad-band pulse of electromagnetic radiation. By doing so, one could determine more precise measurements of the dielectric constants and conductivities of the body. Thus, one may accumulate the reflected and/or transmitted signals to deductively identify influential external sources of non-ionizing radiation that impact the electrical coefficients of incident and scattered fields as a function of position within the body.

2. BACKGROUND

This mathematical investigation directed a fair amount of time and interest to the propagation of electromagnetic pulses in water since a significant proportion of most tissue is water. The water in cells disperses electromagnetic energy due to the ions, unlike the situation with distilled water. Both the dielectric constant, ϵ_r , and the conductivity, σ , of water depend on frequency. For distilled water, this dependency follows that of the curvature in Figures 1A, 1B, 1C and 1D. Please note that the calculated values were

carried out to the fifteenth decimal place, but is not shown on the graphs listed below for readability of the plots.

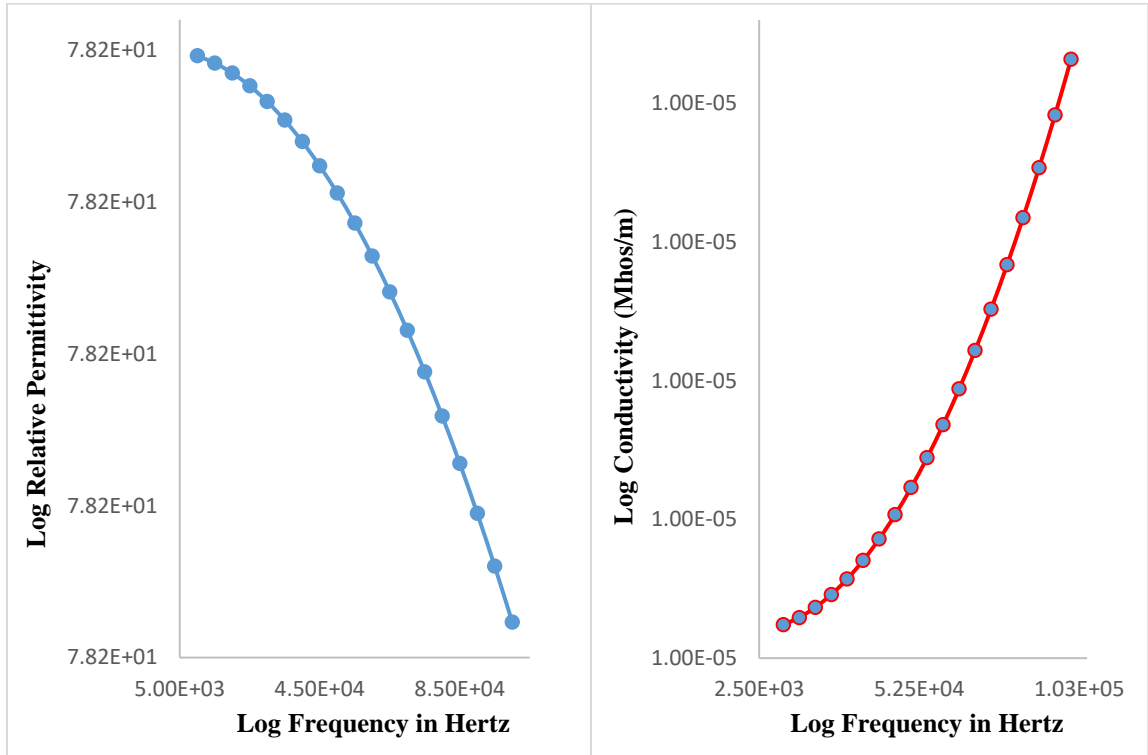


Figure 1.A.: The logarithm to the base ten of the relative permittivity of distilled water is plotted against the logarithm of frequency, 10^4 Hertz.

Figure 1.B.: The logarithm to the base ten of the conductivity is plotted against the logarithm of frequency, 10^4 Hertz.

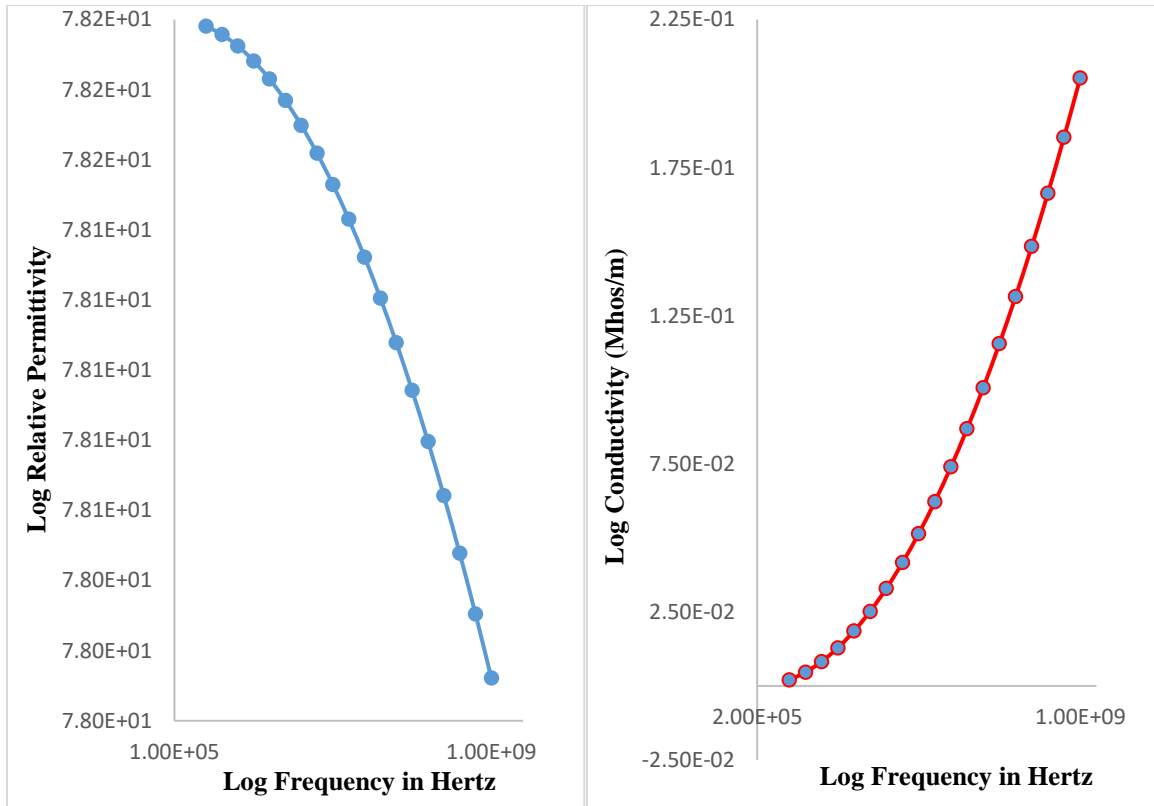


Figure 1.C. The logarithm to the base ten of the relative permittivity of distilled water is plotted against the logarithm of frequency, 10^8 Hertz.

Figure 1.D. The logarithm to the base ten of the conductivity is plotted against the logarithm of frequency, 10^8 Hertz.

At a frequency of 10^4 Hertz and 10^8 Hertz, the trends for both relative permittivity and conductivity have the same behavior. The conductivity increases as the frequency increases. Distilled water has little to no ions present. If distilled water is absent of ions then why does the conductivity increase? This is due to both friction and collision theory. As the frequency increases, this excites the water molecules. The excitation of the water molecules causes them to rotate. The rotation causes friction which generates heat. Think of how a microwave works when it heats up food. The water molecules will also have more kinetic energy as the frequency increases. This kinetic energy will cause the water molecules to collide into one another. Again, creating more heat. The more heat that is produced, the higher the conductivity.

The values calculated for distilled water represent the baseline, or true values. These graphs were computed from the following equations that were provided [8].

$$(1) \quad \varepsilon_r = 5.5 + 72.7 / [1 + (\omega * T)^2]$$

$$(2) \quad \sigma = 10^{-5} + 72.7 * \omega^2 * \varepsilon_o * T / [1 + (\omega * T)^2]$$

These equations are only operational for the frequency range of direct current to 10^{11} Hertz at 25 degrees centigrade. The constant ε_o represents the permittivity of free space, T the so called medium relaxation time with a value of 8.1×10^{-12} seconds, and $\omega = 2\pi f$, where f is the frequency in Hertz. Recall that frequency is generally regarded as the number of times a period or cycle repeats itself over a given period, here in one second. Thus, Hertz may be described as one cycle per second [6]. If in a further investigation of this problem it is desirable to use frequencies greater than 10^{11} Hz, then the calculated data from both the absorption coefficient and the index of refraction needs to be used in concurrence with splines [11]. To carry out this investigation it was important to refer to the half-space geometry that was defined in a previous study. The former investigation's material was based off a square-wave modulated sinusoid oscillating at a selected fixed frequency, with adjustments made for this inquiry [1]. Further discussion of the observed transients dealing with pulse propagations may be found in Reference [14]. An important question addressed in earlier work was whether the dielectric constant and conductivity of a given medium could be determined as a function of frequency from measurements of incident and transmitted pulses [12, 5]. A partial resolution of this question was determined through the implementation of invariant imbedding methods applied to electromagnetic imaging problems. The

resolution of this important question led to further questions. In the case of three-dimensional problems and objects, such as organs and the human body itself, can invariant imbedding be generalized in these cases? Secondly, even though the function is stable, why are the reconstructions sensitive to the presence of additive noise? Finally, under what conditions is a solution unique, and how might a person prove that there is a unique solution of the posed inverse problem?

3. THE INVERSE PROBLEM USING A FREQUENCY RESPONSE FUNCTION

As opposed to the approaches taken to address the previous questions this research focused on a frequency domain analysis technique, rather than that of invariant imbedding. The frequency response function relating incident and transmitted pulses for the given half space geometry is $F(\omega)$.

$$(3) \quad F(\omega) = 2\{\exp[-(\alpha + i\beta)z]\} / [1 + (\beta - i\alpha) / K]$$

Here c = speed of light, $K = \omega/c$, and z is the receiving point within the half-space. The parameters α and β are given by,

$$(4) \quad \alpha = \omega(\mu_0 \varepsilon / 2)^{1/2} * \{-1 + [1 + (\sigma / \omega \varepsilon)^2]^{1/2}\}^{1/2}$$

$$(5) \quad \beta = \omega(\mu_0 \varepsilon / 2)^{1/2} * \{1 + [1 + (\sigma / \omega \varepsilon)^2]^{1/2}\}^{1/2}$$

with $\varepsilon = \varepsilon_r \varepsilon_o$, and μ_o the magnetic permeability of free space [1]. Table I lists some of the values for alpha and beta at certain frequencies by using equations (4) and (5).

Table I. Values of roots Alpha and Beta for the Frequency Response Function

Frequency in Hertz	Alpha, α	Beta, β
$2*10^4$	$2.12694*10^{-4}$	$3.71334*10^{-2}$
$5*10^4$	$2.12996*10^{-4}$	$9.27055*10^{-2}$
$3.5*10^8$	$5.37283*10^{-1}$	64.8693
$7*10^8$	2.14718	129.695

Given a discrete set of angular frequencies, ω_n , $n = 1,2,3 \dots$, determining Fourier Series expansions for the pulses and taking ratios of the appropriate coefficients, the frequency response function can be derived. Specifically, if the transmitted pulse at depth, z , is

$$(6) \quad T(t) = \sum_{n=-\infty}^{\infty} N_n * \exp(i * n * \omega_o * t)$$

with the incident pulse at $z = 0$ is,

$$(7) \quad I(t) = \sum_{n=-\infty}^{\infty} D_n * \exp(i * n * \omega_o * t)$$

then the transfer function, $F(\omega)$ can be calculated as

$$(8) \quad F(\omega_n) = N_n / D_n = X_n + i * Y_n$$

where both $T(t)$ and $I(t)$ are computed in the presence of measurement noise. The values N_n and D_n are complex Fourier coefficients, with $\omega_n = n * \omega_o$, $\omega_o = 2\pi / L$, and L is the period of the pulse. Given that the ratios $X_n + i * Y_n$ are values from measured data, the question becomes whether or not a single α_n, β_n pair can be determined from the relation,

$$(9) \quad X_n + i * Y_n = 2 \{ \exp[-(\alpha_n + i * \beta_n) * z] \} / [1 + (\beta_n - i * \alpha_n) / K_n]$$

For each α_n, β_n pair, ε_n and σ_n may then be determined as,

$$(10) \quad \varepsilon_n = (\beta_n^2 - \alpha_n^2) / \mu_o * \omega_n^2$$

$$(11) \quad \sigma_n = 2 * \alpha_n * \beta_n / \mu_o * \omega_n$$

The following equations are derived from equation (9)

$$(12) \quad X_n + X_n * \beta_n / K_n + Y_n * \alpha_n / K_n + 2[\cos(\beta_n * z)] * \exp(-\alpha_n * z) = 0$$

$$(13) \quad Y_n + Y_n * \beta_n / K_n - X_n * \alpha_n / K_n + 2[\sin(\beta_n * z)] * \exp(-\alpha_n * z) = 0$$

Using equations (12) and (13) one can then calculate the values for both X_n and Y_n , which will be used later on. Table II gives some examples of the values calculated for both X_n and Y_n .

Table II. Values of X_n and Y_n at Given Frequencies

Frequency in Hertz	X_n	Y_n
$2.5 \cdot 10^4$	$1.02117 \cdot 10^{-2}$	$2.47730 \cdot 10^{-1}$
$6.5 \cdot 10^4$	$3.94534 \cdot 10^{-3}$	$2.48408 \cdot 10^{-1}$
$3.5 \cdot 10^4$	$1.84941 \cdot 10^{-3}$	$2.48540 \cdot 10^{-1}$
$9.5 \cdot 10^4$	$5.01657 \cdot 10^{-3}$	$2.48626 \cdot 10^{-1}$

A bit of algebraic manipulation of the given two coupled equations, leads to the following identities.

$$(14) \quad (D1_n / 2) * \alpha_n * \exp(\alpha_n * z) = K_n * \sin(\beta_n * z + D2_n)$$

$$(15) \quad z^{-1} (1 + \beta_n / K_n)^{-1} * \cos(\beta_n * z + D2_n) * \ln\{2 * D1_n^{-1} (1 + \beta_n / K_n)^{-1} * \cos(\beta_n * z + D2_n)\} \\ = K_n * \sin(\beta_n * z + D2_n)$$

where

$$(16) \quad D1_n = (X_n^2 + Y_n^2)^{1/2}$$

$$(17) \quad D2_n = \arctan(Y_n / X_n)$$

$$(18) \quad \alpha_n = z^{-1} * \ln[2 * D1_n^{-1} (1 + \beta_n / K_n)^{-1} * \cos(\beta_n * z + D2_n)]$$

Implementing equation (15) one can solve for the parameter β_n . From equations (4) and (5) it is not difficult to assert that both $\alpha_n > 0$ and $\beta_n > 0$. The search for roots β_n of (15) may be narrowed using the inequality.

$$(19) \quad 2k\pi \leq (\beta_n * z + D2_n) < (2k + \frac{1}{2}) * \pi$$

and given that $k = 0, 1, 2, 3, \dots k_{\max}$. For each value of k , there can only be one root. It is important to note that the parameter, β_n , is bounded below by zero and above by the condition that $2 * D1_n^{-1} (1 + \beta_n / K_n)^{-1}$ is greater than or equal to one. Thus, there must be a finite number of values for β_n , if any. When the depth, z , is zero then equation (15) has the unique solutions,

$$(20) \quad \beta_n = K_n * (2 * D1_n^{-1} * \cos(D2_n) - 1)$$

and

$$(21) \quad \alpha_n = 2 * K_n * D1_n^{-1} * \sin(D2_n)$$

These equations indicate that for a rare and distinct arrangement of both frequency and transmission depth, there is a unique determination of ϵ and σ . Below, Table III shows the new values for both alpha and beta in comparison to Table I.

Table III. Values of roots Alpha and Beta from Equation 15

Frequency in Hertz	Alpha, α_n	Beta, β_n
$2*10^4$	$-3.38329 * 10^{-3}$	$2.78905*10^{-3}$
$5*10^4$	$2.99354*10^{-3}$	$-9.02382*10^{-3}$
$3.5*10^8$	-58.4220	-26.2210
$7*10^8$	-87.9775	103.352

Derivation on how to obtain equation (20). From equation (15) multiply both sides of the equation by z.

$$(1 + \beta_n / K_n)^{-1} * \cos(\beta_n * z + D2_n) * \ln\{2 * D1_n^{-1} (1 + \beta_n / K_n)^{-1} * \cos(\beta_n * z + D2_n)\} \\ = K_n * \sin(\beta_n * z + D2_n) * z$$

Let $z = 0$,

$$(1 + \beta_n / K_n)^{-1} * \cos(D2_n) * \ln\{2 * D1_n^{-1} (1 + \beta_n / K_n)^{-1} * \cos(D2_n)\} = 0$$

Dividing both sides by $(1 + \beta_n / K_n)^{-1} * \cos(D2_n)$,

$$\ln\{2 * D1_n^{-1} (1 + \beta_n / K_n)^{-1} * \cos(D2_n)\} = 0$$

The next step is to transform away the natural log through the use of exponentiation. This produces,

$$2 * D1_n^{-1} (1 + \beta_n / K_n)^{-1} \cos(D2_n) = 1$$

To solve for beta, multiply both sides by $D1_n(1 + \beta_n / K_n)$.

$$2 * \cos(D2_n) = D1_n(1 + \beta_n / K_n)$$

To isolate beta, divide by $D1_n$ and subtract the one reducing the equation to,

$$(2 * \cos(D2_n) / D1_n) - 1 = (\beta_n / K_n)$$

Multiplication of both sides by K_n isolates beta, giving equation (20).

$$\beta_n = K_n * (2 * D1_n^{-1} * \cos(D2_n) - 1)$$

4. NUMERICAL RESULTS FOR THE NOISELESS CASE

From the original figures provided by [1], it was concluded that at lower frequencies, unique values for the dielectric constant and conductivity exist, however, multiple roots can occur above a given frequency. The graphs provided follow the same trend as those of distilled water, but the roots greatly increased as the frequency increased. If the observation point, z , is shifted more towards the half-space surface, then the number of roots multiplied in number as the frequency was amplified.

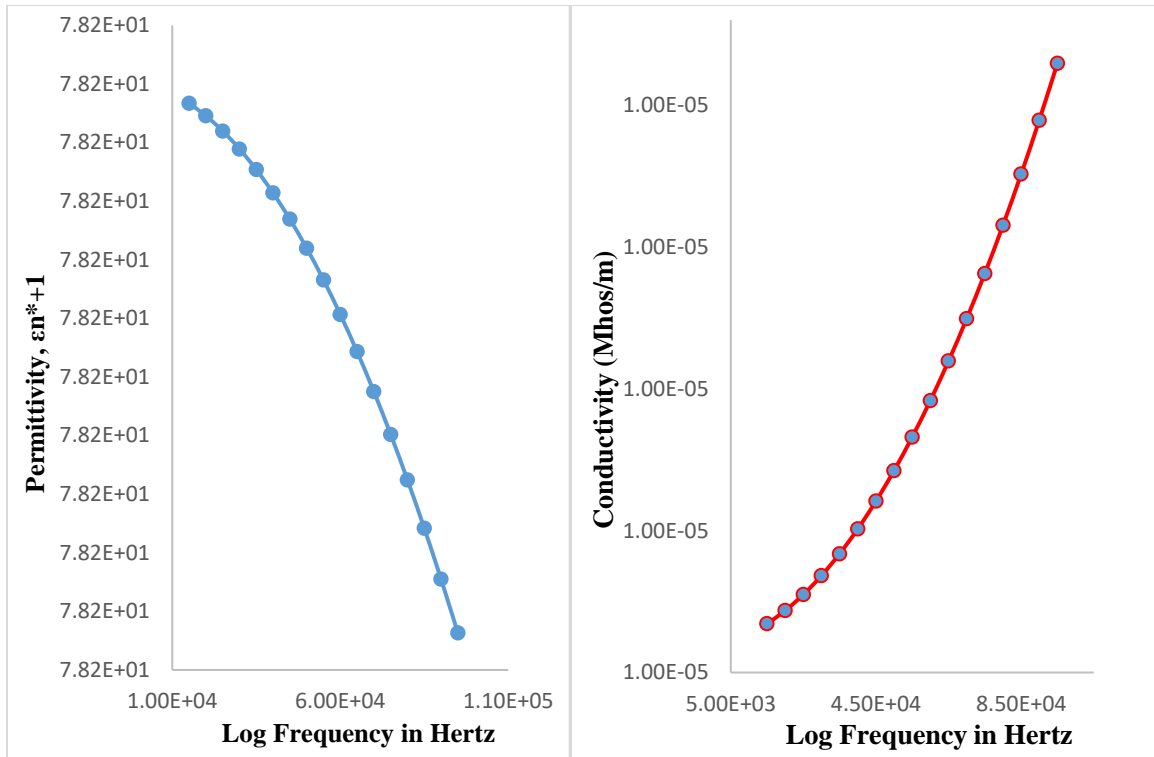


Figure 2.A. The logarithm to the base ten of the relative permittivity of the noiseless case is plotted against the logarithm of frequency, 10^4 Hertz.

Figure 2.B. The logarithm to the base ten of the conductivity of the noiseless case is plotted against the logarithm of frequency, 10^4 Hertz.

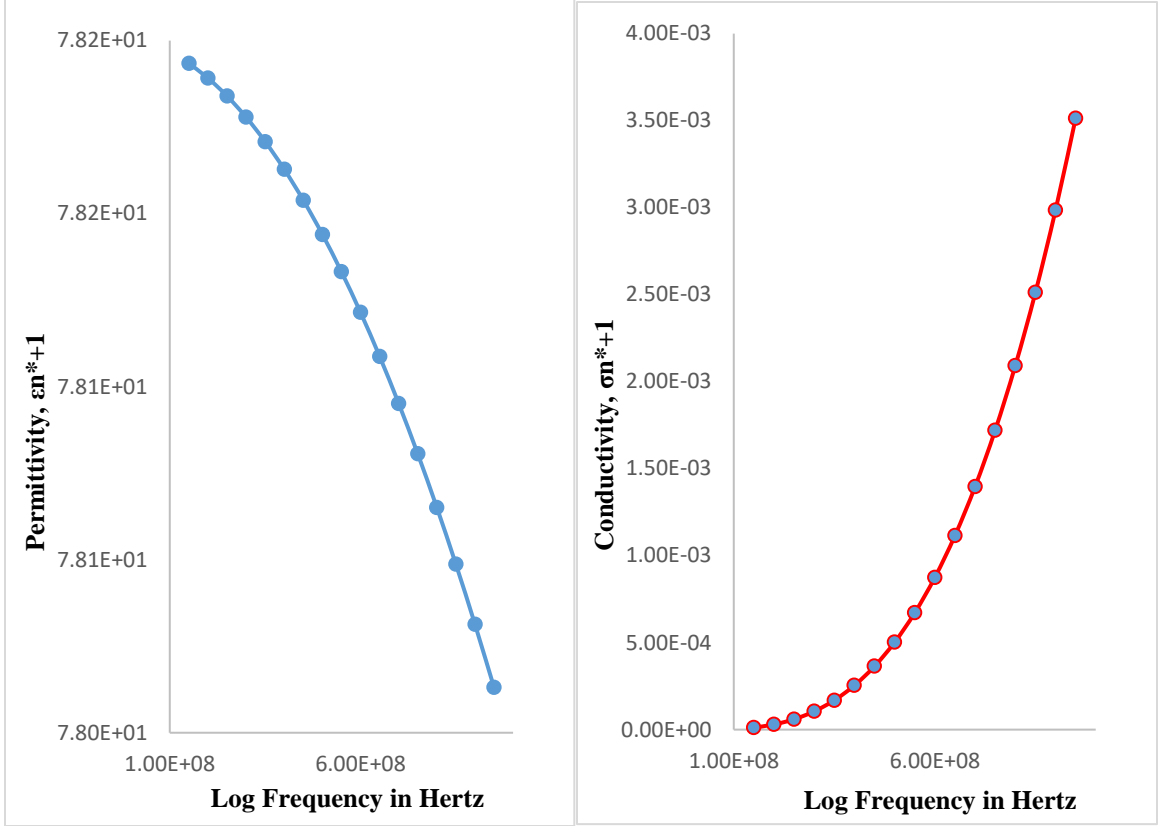


Figure 2.C. The logarithm to the base ten of the relative permittivity of the noiseless case is plotted against the logarithm of frequency, 10^4 Hertz.

Figure 2.D. The logarithm to the base ten of the conductivity of the noiseless case is plotted against the logarithm of frequency, 10^4 Hertz.

The results suggest it would be of interest to move from the area where unique values exist to the regions where there are multiple roots in order to determine further estimates for $\epsilon(\omega)$ and $\sigma(\omega)$. For the noiseless case, the numerical procedure is to calculate the associated $\epsilon_{n,k}, \sigma_{n,k}$ values by root finding, where k runs from one through k_{\max} . The value k_{\max} is the maximum number of complex roots of equation (15) for each frequency of the incident and transmitted pulses.

$$(22) \quad \hat{\epsilon}_{n^*+1} = \epsilon_{n^*} + [(\epsilon_{n^*} - \epsilon_{n^*-1}) / (\omega_{n^*} - \omega_{n^*-1})] * (\omega_{n^*+1} - \omega_{n^*})$$

$$(23) \quad \hat{\sigma}_{n^*+1} = \sigma_{n^*} + [(\sigma_{n^*} - \sigma_{n^*-1}) / (\omega_{n^*} - \omega_{n^*-1})] * (\omega_{n^*+1} - \omega_{n^*})$$

Equations (22) and (23) are essentially discrete versions of Newton's Method. The values of ε_{n^*+1} , σ_{n^*+1} are then chosen as the $\varepsilon_{n^*+1,k}$, $\sigma_{n^*+1,k}$ pair closest to $\hat{\varepsilon}_{n^*+1}$, $\hat{\sigma}_{n^*+1}$. This numerical procedure recovered ε and σ values specified by equations (1) and (2) through the region of multiple roots when values of ω were sufficiently close. It is important to note that the continuation only uses the first derivative. The algorithm that chose the n^*+1 root to be that root nearest to the n^* root worked well, but the least squared values were greater in comparison to those computed using the first derivative. Listed in Table IV are the values for both the dielectric constant and conductivity from use of the algorithm for the noiseless case. One can see that the values for the dielectric constant do not greatly alter, and only show a slight change as the frequency is increased. Again, for the conductivity values there is not much change at a frequency of 10^4 Hertz until the fifth and sixth decimal place which is not shown on the table. However, one can see that when the frequency is 10^8 Hertz, the values for conductivity are far from the true value. This might be due to the lack of stabilization that noise provides. The original values were carried out to the fifteenth decimal place, but to have the figures fit this article format the values were changed to scientific notation.

Table IV. Values of Dielectric Constant and Conductivity in the Noiseless Case using the Algorithm

Frequency (Hz)	True ϵ	Relative ϵ	True σ ($\mu\text{mhos/m}$)	Relative σ ($\mu\text{mhos/m}$)
$3.5 \cdot 10^4$	78.2	78.2	10.0	10.0
$4 \cdot 10^4$	78.2	78.2	10.0	10.0
$1.5 \cdot 10^8$	78.1	78.2	4,640	11.9
$6 \cdot 10^8$	78.0	78.1	74,000	875

5. NUMERICAL RESULTS WITH NOISE

Using the representation provided by [3], in-band noise was added to both the incident and transmitted signals. These self-governing signals of the form

$$(24) \quad \xi^{(i)}(t) = \sum_{n=1}^N [a_n^{(i)} * \sin(\omega_n * t) + b_n^{(i)} * \cos(\omega_n * t)]$$

were added to the signals. From a Gaussian distribution with a mean zero, and a standard deviation chosen to be constant across the entire frequency range, one can derive the coefficients a_n and b_n which are independent random variables. To calculate the percentage of noise to signal ratio used, one divides $\text{STD}(\xi)$ by the peak of the noiseless incident signal, where,

$$(25) \quad \text{STD}(\xi)^2 = \lim_{T \rightarrow \infty} \left\{ \frac{1}{2T} \int_{-T}^T \xi(t)^2 dt \right\}$$

The value T is the transmitted pulse with higher values of the pulse implemented as T is approaching infinity. Further or more elaborate investigations should be implemented in the evaluation of this equation if more trial runs are used. The percentage of the presence of the added noise is very small and is applied for stabilization.

In the following table, values for the dielectric constant and the conductivity presented are such that frequencies with single roots from equation (15) are considered. The effect of noise on the continuation process has not yet been explored in the given research project. For some of the given examples it can be noted in Table V, note that no realistic roots exist, despite the very weak additive noise.

Observing the given calculated estimates, it seems that the values for the dielectric constant appear to be acceptable for they are close to the accepted value, but the values for the conductivity appear to vary greatly, especially as the frequency increases. At the frequency levels of both 10^4 and 10^8 Hertz the dielectric constant is close to the true expected value, but the permittivity appears to fluctuate greatly. Out of mere interest, another investigative run was taken at a frequency of 10^{10} Hertz, and the values for the conductivity were more variable and had more fluctuations when plotted. This suggests that the equations start to lose their authenticity as the frequency is increased. It is possible that the half-space geometry needs to be re-evaluated for different depths of z . One might also consider trying a different type of modulated sinusoidal wave. With microelectronic circuits, it is very common for one to use a square-wave. This same approach was implemented for this investigation since it mimics an inverse problem where one would turn the pulse on and off. From Table V, even the true dielectric constant values do not change much as the frequency increases, but the conductivity

values of distilled water increase greatly as the frequency increases. This follows the natural tendency for conductivity to decrease overall as frequency increases, as it does in the graphs. Conductivity tends to decrease with decreasing concentration, alternately it tends to increase with increasing temperature. The values for conductivity when noise is present tend to be far from the true value with great variation as illustrated by the computed values displayed in the table. This could be due to a rounding error in the programs used. It could also be due to not using enough trial runs, and the appropriate interval step sizes. Another possible reason why the values for conductivity have variation when noise is present might be due to the fact that noise may cause a resonating vibration with the water molecules. This vibration creates more kinetic energy and collisions, therefore producing more friction and heat. The more heat produced, the greater the conductivity.

Table V. Identification of Tissue Properties in the Presence of Noise

Frequency (Hz)	True ϵ	Relative ϵ	True σ ($\mu\text{mhos/m}$)	Relative σ ($\mu\text{mhos/m}$)
$3.5 \cdot 10^4$	78.2	78.2 +/- 0.13	10.0	10.0 +/- 9.9
$4 \cdot 10^4$	78.2	78.2 +/- 0.13	10.0	10.0 +/- 9.9
$1.5 \cdot 10^8$	78.1	78.2 +/- 0.85	4,640	2,389 +/- 994.8
$6 \cdot 10^8$	78.0	78.2 +/- 671	74,000	174,963 +/- 976.4

6. CONCLUSION

When the frequency response function and root finding method is in accord, then the values of ω between zero and a limiting value of ω can be determined. If both $\epsilon(\omega)$ and $\sigma(\omega)$ are differentiable, then the $\epsilon(\omega)$ and $\sigma(\omega)$ determinations can be calculated above the ω^* limit, even in the absence of noise for this investigation's model. Multiple quantitative values for $\epsilon(\omega)$ and $\sigma(\omega)$ can be acquired above ω^* which will reconfigure the incident pulse.

Since living tissue cannot generate energy, even though it is a linear medium, one must be cautiously skeptical to assume that its electromagnetic response can be simply overseen by a linear ordinary differential equation and can therefore be described by differentiable functions $\epsilon(\omega)$ and $\sigma(\omega)$. In terms of electromagnetic propagation with respect to living tissue, the tissue tends to be causal; but this property is not enough to guarantee the differentiability of both $\epsilon(\omega)$ and $\sigma(\omega)$. Referring to the theorem which indicates that the Fourier transform, $F(\omega)$ of a causal function $f(t)$, in the upper half-plane, is holomorphic, one then has that the function would be infinitely differentiable [19]. However, in the limit as v approaches 0^+ , the frequency response function is not differentiable, with v a real variable [13, 19]. Due to this basis of causality, one should not assume differentiability.

From the view of a dielectric response, living tissue is an unknown structure. Therefore, it would be pragmatic to be cautious with respect to the assumptions that were made for $\epsilon(\omega)$ and $\sigma(\omega)$. Especially regarding the kernel of the linear operator that governs the tissue response. Ergo, it is important to tentatively conjecture that the

algorithm for the frequency response function, determined through resolution of the inverse problem has a unique solution only when signals are used that have a frequency below a critical frequency. The critical frequency is dependent on the physical dimensions of the structure that is to be studied [1]. If it is assumed that both $\epsilon(\omega)$ and $\sigma(\omega)$ are differentiable then a unique determination can be expected at higher frequencies. The overall goal for this experimnt in the future would be to illuminate the human body with a broad-band pulse of electromagnetic radiation. One could determine more accurate estimates of the dielectric constants and conductivities of the body by accumulating reflected and/or transmitted signals. The signals may then be implemented to deductively conclude incident and scattered fields of the body as a function of position within the body. This paper describes a few of the initial steps toward this ultimate overarching meaninfgul goal.

REFERENCES

- [1] Albanese, R., Penn, J., Medina, R. (1989, September). *Short-rise time Microwave Pulse Propagation through Dispersive Biological Media*, Journal of the Optical Society of America A, Vol. 6, No. 9, pp. 1441-1446.
- [2] Arcangeli, G., Lombardini, P.P., Lovisolo, G.A., Marsiglia, G., Piatelli, M. (1984, January). *Focusing on 915 Mhz Electromagnetic Power on Deep Human Tissues: A Mathematical Model Study*, IEEE Transactions on Biomedical Engineering, Vol BME-31, No. 1, pp. 47-52.
- [3] Bendat, J.S. (1958). *Principles and Applications of Random Noise Theory*, John Wiley and Sons, Inc., New York.
- [4] Burdette, E.C., Cain, F.L., Seals, J. (1980, April). *In Vivo Probe Measurements Technique for Determining Dielectric Properties at VHF Through Microwave Frequencies*, IEEE Transactions on Microwave Theory and Techniques, Vol MTT-28, No. 4, pp. 414-427.
- [5] Coronas, J., Krueger, R. (1983). *Obtaining Scattering Kernels Using Invariant Imbedding*, Journal of Mathematical Analysis and Applications, Vol. 95, pp. 393-415.
- [6] “Electrical Waveforms”. (n.d.). Retrieved from <https://www.electronics-tutorials.ws/waveforms/waveforms.html>
- [7] Grant, E.H., Sheppard, R.J., South, G.P. (1978). *Dielectric Behaviour of Biological Molecules in Solution*, Clarendon Press, Oxford.
- [8] Grant, E.H., (1988). King’s College, Univeristy of London, London, UK. See also Grant, E.H., Sheppard, R.J., South, G.P. (1978). *Dielectric Behaviour of Biological Molecules in Solution*, Clarendon Press, Oxford.
- [9] Hahn, G.M., (1984, January). *Hyperthermia for the Engineer: A Short Biological Primer*, IEEE Transactions on Biomedical Engineering, Vol BME-31, No. 1, pp. 3-8.
- [10] “Hyperthermia to Treat Cancer”. (2016, May 3). Retrieved from <https://www.cancer.org/treatment/treatments-and-side-effects/treatment-types/hyperthermia.html>
- [11] Jackson, J.D. (1975). *Classical Electrodynamics*, John Wiley & Sons, New York.

- [12] Krueger, R.J. (1981, December). *Induced Field Structures in Heterogeneous Bodies by Electromagnetic Pulses*, Final Report of USAF Contract F33615-78-D-0629 0030.
- [13] Nussenzveig, H.M. (1972). *Causality and Dispersion Relations*, Academic Press, New York.
- [14] Oughstun, K.E., Sherman, G.C. (1990, June 1). *Uniform Asymptotic Description of Ultrashort Rectangular Optical Pulse Propagation in a Linear, Casually Dispersive Medium*, Physical Review A, Vol. 41, No. 11, pp.6090-6113.
- [15] “Power Lines, Electrical Devices and Extremely Low Frequency Radiation”. (2017, April 18). Retrieved from <https://www.cancer.org/cancer/cancer-causes/radiation-exposure/extremely-low-frequency-radiation.html>
- [16] “Shattering Cancer with Resonant Frequencies”. (2015, Oct 21). Retrieved from <https://www.apastyle.org/learn/faqs/web-page-no-author.html>
- [17] Steel, M., Sheppard, R.J., Grant, E.H., (1984). *A Precision Method for Measuring the Complex Permittivity of Solid Tissue in the Frequency Domain between 2 and 18GHz*, Journal of Physics Series E: Scientific Instruments, Vol 17, pp. 30-34.
- [18] Tell, R.A. (1980, January). *Population Exposure to VHF and UHF Broadcast Radiation in the United States*, Proceedings of the IEEE, Vol 68, No. 1, pp. 6-12.
- [19] Titchmarsh, E.C. (1948). *Introduction to the Theory of Fourier Integrals*, Clarendon Press, Oxford.
- [20] Violette, J.L.N., White, D.R.J., Violette, M.J. (1987). *Electromagnetic Computability Handbook*, Van Nostrand Reinhold Compnay, New York.
- [21] Weaver, J. B. (2013, Sep 18). Retrieved from <https://www.ncbi.nlm.nih.gov/pmc/articles/PMC3776477/>
- [22] “What are electromagnetic fields?”. (2019). Retrieved from <https://www.who.int/peh-emf/about/WhatisEMF/en/index1.html>
- [23] “What is non-ionising radiation?”. (n.d.). Retrieved from <https://www.arpansa.gov.au/understanding-radiation/what-radiation/what-non-ionising-radiation>